Liquid Crystals
Publication details, including instructions for authors and subscription information:
http://www.informaworld.com/smpp/title~content=t713926090

Magnetite nanoparticles/chiral nematic liquid crystal composites with magnetically addressable and magnetically erasable characteristics

Wang Hu[a]; Haiyan Zhao[a]; Liankun Shan[b]; Li Song[a]; Hui Cao[a]; Zhou Yang[a]; Zihui Cheng[a]; Chunzhu Yan[b]; Sijin Li[a]; Huai Yang[a]; Lin Guo[b]
[a] Department of Materials Physics and Chemistry, School of Materials Science and Engineering, University of Science and Technology Beijing, Beijing, China [b] School of Chemistry and Environment, Beijing University of Aeronautics and Astronautics, Beijing, China

Online publication date: 28 May 2010

To cite this Article Hu, Wang , Zhao, Haiyan , Shan, Liankun , Song, Li , Cao, Hui , Yang, Zhou , Cheng, Zihui , Yan, Chunzhu , Li, Sijin , Yang, Huai and Guo, Lin(2010) 'Magnetite nanoparticles/chiral nematic liquid crystal composites with magnetically addressable and magnetically erasable characteristics', Liquid Crystals, 37: 5, 563 — 569
To link to this Article: DOI: 10.1080/02678291003710441
URL: http://dx.doi.org/10.1080/02678291003710441

Liquid Crystals,
Vol. 37, No. 5, May 2010, 563–569

Taylor & Francis
Taylor & Francis Group

Magnetite nanoparticles/chiral nematic liquid crystal composites with magnetically addressable and magnetically erasable characteristics

Wang Hu[a], Haiyan Zhao[a], Liankun Shan[b], Li Song[a], Hui Cao[a], Zhou Yang[a], Zihui Cheng[a], Chunzhu Yan[b], Sijin Li[a], Huai Yang[a]* and Lin Guo[b]*

[a]*Department of Materials Physics and Chemistry, School of Materials Science and Engineering, University of Science and Technology Beijing, Beijing 100083, China;* [b]*School of Chemistry and Environment, Beijing University of Aeronautics and Astronautics, Beijing 100083, China*

(*Received 8 December 2009; final version received 17 February 2010*)

A magnetite (Fe_3O_4) nanoparticle/chiral nematic liquid crystal (N*-LC) composite was prepared and filled into a planar treated cell. The Fe_3O_4 nanoparticles had been modified by oleic acid so that they could be better dispersed in the composite. When a magnetic field was scanned on the outer surface of the cell locally, Fe_3O_4 nanoparticles moved towards the inner surface of the cell correspondingly, and the black expected information was displayed. When the magnet was applied to the opposite outer surface, the information was erased. After polymer network walls were prepared in the composite, the resolution of the information displayed increased. Then, through the formation of hydrogen bonds between the nanoparticles and chiral pyridine compound (CPC) doped in the composite, the pitch length of the N*-LC could be adjusted by altering the intensity of the applied magnetic field. The composite doped with CPC could potentially be used as a material for a type of reflective colour paper with magnetically controllable characteristics.

Keywords: chiral nematic liquid crystals; selective reflection; hydrogen bond; pitch

1. Introduction

Recently, much effort has been devoted to preparing electronic paper (E-paper), especially for producing colour display with a low power consumption. Generally, there are two kinds of mechanisms used in the traditional study, one of which is based on the electrophoretic motion of microparticles inside small capsules, and the other on the rapid manipulation of electrowetting on a micrometre scale [1, 2]. The materials thus prepared demonstrated the characteristics of fast response, flexibility, high contrast and are easy to fabricate in large areas. On the other hand, liquid crystal (LC), a traditional material used for display, has also attracted much interest for its applications in E-paper. For example, it can be used to prepare an electrically addressable and electrically erasable display device, in this case, the nematic liquid crystal (N*-LC) can be changed between a planar and focal conic texture by applying electric fields with different frequencies [3, 4]. Meanwhile, the thermally addressable and electrically erasable N*-LC devices, as well as the electrically addressable and thermally erasable ones, have also been studied [5–7]. Moreover, due to the interaction of polymer networks and LC molecules, polymer-stabilised N*-LCs have also been devoted to applications of E-paper, which can exhibit black and white display with grey scale potential, as well as having flexible characteristics [8–11]. However, the materials mentioned above can only be used for black and white display. Due to the self-organised, periodic helical structure of the molecules of N*-LC, which exhibits the selective reflection characteristics [12], the colour change achieved by changing the external factors including electric field, temperature and light irradiation, can also be used in reflective colour paper [13–19]. However, the reflective colour of LC materials with magnetically controllable characteristics has seldom been reported.

Our objective was to provide a simple new way of realising the magnetochromic effect by the combination of LC and nanoparticles with a low intensity of the driving magnetic field. We studied the magneto-optical properties of a magnetite (Fe_3O_4) nanoparticle/N*-LC composite and demonstrated that this composite exhibits magnetically addressable and magnetically erasable characteristics, especially the magnetochromic characteristics, which have great potential in magnetic paper (M-paper, where information can be magnetically addressed and erased), especially in reflective colour M-paper.

An N*-LC can be formed when a nematic LC is doped with a chiral dopant. In an N*-LC phase, the long axis of the LC molecule rotates about a helix. The pitch length, P, of the helix, corresponding to a 2π

*Corresponding authors. Email: yanghuai@mater.ustb.edu.cn; guolin@buaa.edu.cn

ISSN 0267-8292 print/ISSN 1366-5855 online

DOI: 10.1080/02678291003710441
http://www.informaworld.com

molecular rotation, is determined by the concentration of the chiral dopant, which decreases with increasing fraction of chiral dopant. A single-pitch N*-LC selectively reflects the light of wavelength between $\lambda_{max} = Pn_o$ and $\lambda_{max} = Pn_e$. Here, n_o and n_e are the ordinary and extraordinary refractive indexes of the locally uniaxial structure, respectively. The bandwidth of the selective reflection spectrum $\Delta\lambda$ is given by $\Delta\lambda = \lambda_{max}–\lambda_{max} = (n_e–n_o)P = \Delta nP$. Here, $\Delta n = n_e–n_o$ is the birefringence [12, 20]. Within this reflection region, right (left) circularly polarised light is reflected by a right (left)-handed helix, whereas left (right) circularly polarised light is transmitted. Outside the reflection band, both polarisation states are transmitted. Based on this principle, the expected M-paper can exhibit colour display without backlight.

2. Experimental details

2.1 Materials

In this study, a nematic LC, SLC1717 (Slichem Liquid Crystal Material Co. Ltd, Shijiazhuang, China), chiral dopants, S811 (Merck Co. Ltd) and a chiral pyridine compound (CPC) (TCI Co. Ltd, Ningbo City, China), a photopolymerisable LC monomer, C6M, a photoinitiator, IRG 651 (TCI Co. Ltd) and the synthesised Fe_3O_4 nanoparticles were used. The chiral dopants were both left-handed. Fe_3O_4 nanoparticles were synthesised using a chemical coprecipitation method and then modified by oleic acid. C6M was laboratory-synthesised [21]. The chemical structures of the materials used are listed in Figure 1 and the compositions and weight ratios of the five studied samples are listed in Table 1.

2.2 Synthesis of Fe_3O_4 nanoparticles

$FeCl_3$ 0.20 mol L^{-1} (10 ml) was slowly added to a 0.15 mol L^{-1} $FeCl_2{\cdot}4H_2O$ (10 ml) solution. The mixture was heated to 65°C under a flow of nitrogen and mechanical stirring (500 rpm) for 30 min. Tetramethylammonium hydroxide ($N(CH_3)_4OH$) 0.50 mol L^{-1} (70 ml) was slowly added to the mixture. Vigorous stirring was continued for 1 h at 65°C. The black mixture was cooled to room temperature by removing the heat source. Under ambient conditions, ethanol (50 ml) was added to the mixture and a black material was precipitated and separated via centrifugation. The product, Fe_3O_4 nanoparticles, was then dissolved and washed with ethanol by ultrasonic dispersion, and centrifuged (6000 rpm, 10 min) to remove the solvent. This procedure was repeated five times, and the product was dried under vacuum for about 24 h.

Table 1. The compositions and weight ratios of samples 1–5.

Sample	SLC1717/S811/unmodified Fe_3O_4/modified Fe_3O_4/C6M/ IRG 651/chiral pyridine compound (wt%)
1	66.3/25.7/8.0/–/–/–/–
2	66.3/25.7/–/8.0/–/–/–
3	64.6/25.1/–/8.0/2.2/0.1/–
4	65.1/20.2/–/8.0/2.2/0.1/4.4
5	61.3/23.7/–/8.0/2.2/ 0.1/4.7

2.3 Modification of Fe_3O_4 nanoparticles

The Fe_3O_4 nanoparticles (1 mmol) were dissolved in tetrahydrofuran (THF) (20 ml) and the mixture was heated to 65°C under a flow of nitrogen and mechanical stirring (500 rpm) for about 30 min. A solution of oleic acid (0.50 ml) (TCI Co. Ltd) in THF (10 ml) was added to the heated solution. Then the oleic acid (0.2 ml) was added repeatedly five times into the mixture, with intervals of 5 min. The mixture was heated to 85°C to reflux for 2 h with mechanical stirring (1000 rpm). The black mixture was cooled to room temperature by removing the heat source. Under ambient conditions, ethanol (50 ml) was added to the mixture and a black material was precipitated and separated via centrifugation. The black product was dissolved in hexane in the presence of oleic acid (0.2 ml). Centrifugation (6000 rpm, 10 min) was applied to remove any undispersed residue. The product, oleic acid-coated Fe_3O_4 nanoparticles, was then dissolved and washed with ethanol by ultrasonic dispersion and centrifuged (6000 rpm, 10 min) to remove the solvent. This procedure was repeated five times, and the product was dried under vacuum for 24 h.

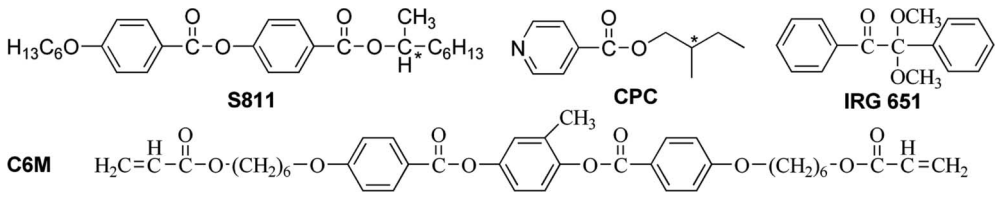

Figure 1. Chemical structures of the materials used.

2.4 Preparation of the samples

To obtain homogeneous alignment, a 2.0 wt% polyvinyl alcohol aqueous solution was coated on to the inner surfaces of the substrates of cells by spin casting. The deposited film was dried at 80°C for about 30 min, and subsequently rubbed with a textile cloth under a pressure of 2 g cm^{-2} along one direction. Polyethylene terephthalate films, 75 μm thick, were used as spacers of the cell. The studied samples were dissolved in acetone, stirred for about 2 h and then the acetone was evaporated completely under vacuum. Finally, the prepared sample was filled into the cell by capillary action in the temperature range of the cholesteric phase.

2.5 Measurements

The X-ray diffraction (XRD) curve of the prepared Fe_3O_4 nanoparticles was obtained by a Rigaku X-ray diffractometer (Rigaku Goniometer PMG-A2, CN2155D2, wavelength = 0.15147 nm) with Cu Kα radiation. The morphology of the Fe_3O_4 nanoparticles was observed by a field emission scanning electron microscope (SEM) (Supra 55). Micrographs of the Fe_3O_4 nanoparticles in the N*-LC were observed by polarising optical microscopy (POM) (Olympus BX51). The Fe_3O_4 nanoparticles before and after modification were laminated directly with potassium bromide and analysed with an infrared (IR) spectrometer (Perkin Elmer Spectrum 100, Waltham, MA, USA) between 500 and 4000 cm^{-1}, respectively. The spectra of selective reflection were obtained by UV/VIS/NIR spectrophotometer (JASCO V-570). The microstructure of the polymer network was observed by SEM (Cambridge S250) with the samples coated with a thin layer of carbon to eliminate any problems of electric charge.

3. Results and discussion

Figure 2 shows the XRD curve of the Fe_3O_4 nanoparticles, the IR spectra and the SEM images of the unmodified and modified nanoparticles, and the POM micrographs of samples 1 and 2. Figure 2(a) indicates the successful preparation of nanoparticles since the positions and relative intensities of all the diffraction peaks matched well with the diffraction data of the standard Fe_3O_4 powder [22]. Figure 2(b) shows the IR spectra of both of the unmodified Fe_3O_4 nanoparticles (spectrum 1) and the modified ones (spectrum 2). The reasons for the modification of the Fe_3O_4 nanoparticles were as follows. If the size of Fe_3O_4 nanoparticles is more than 7 nm, they are easy to get blocked in the LCs [23]. The size of the Fe_3O_4 nanoparticles synthesised here was about 50 nm, so the modification with organic materials was necessary to achieve a uniform distribution in the LC. In spectrum 1, the absorption at 1635 cm^{-1} was assigned to the C–N stretching vibration band, which results from the reactant of $N(CH_3)_4OH$ during the preparation of the nanoparticles. This indicates the adsorption of $N(CH_3)_4OH$ on Fe_3O_4 [24]. In spectrum 2, the absorption around 2922 and 2851 cm^{-1} indicated the existence of $–CH_2–$ groups and that around 1055, 1450, 1527 and 1628 cm^{-1} indicated the existence of –COO– groups in the coated Fe_3O_4 nanoparticles, which showed that modification of the nanoparticles had been achieved [25–28]. However, the absorption around 3429 cm^{-1} indicated that there were still some –OH groups that had not yet reacted on the surface of the Fe_3O_4 nanoparticles. Compared with spectrum 1, the ratio of peak area at 3429 cm^{-1} resulting from –OH groups to that at 580 cm^{-1} from Fe–O groups decreased somewhat, implying that parts of the –OH groups are involved in the chemical reaction for the modification. Figure 2(c) shows the typical SEM image of representative 50-nm unmodified Fe_3O_4 nanoparticles, while Figure 2(d) shows that of the modified nanoparticles. Comparing Figure 2(c) and (d), it can be inferred that surface modification is quite beneficial to the distribution of the nanoparticles. Figure 2(e) and (f) shows the POM micrographs of the unmodified Fe_3O_4 nanoparticles and the modified ones in the N*-LC (samples 1 and 2), respectively. It can be seen clearly that the modified nanoparticles disperse much more homogeneously than the unmodified ones in the N*-LC. In Figure 2(f), under POM, the agglomeration of the modified nanoparticles is hard to observe. This is due to the fact that the organic ligands could not only prevent the agglomeration of the nanoparticles, but also improve the distribution of the nanoparticles in the LC, which also contributed to the formation of a stable distribution system [29]. Moreover, by comparing Figure 2(e) and (f), it can also be seen that less agglomeration of the nanoparticles is helpful for the formation of the planar texture of N*-LC , which is quite beneficial to improve the reflective effect of the N*-LC.

Figure 3(a)–(c) illustrates the mechanism for the preparation of the expected material. Initially, the black modified Fe_3O_4 nanoparticles disperse in the N*-LC, which exhibits a background colour if the reflecting wavelength is within the wavelength range of visible light as shown in Figure 3(a). If a magnet block is placed on the surface of substrate A of the cell, the Fe_3O_4 nanoparticles will move to the inner surface of substrate A and the local region of the cell appears black as shown in Figure 3(b). Thus, a black pattern (information) can be addressed

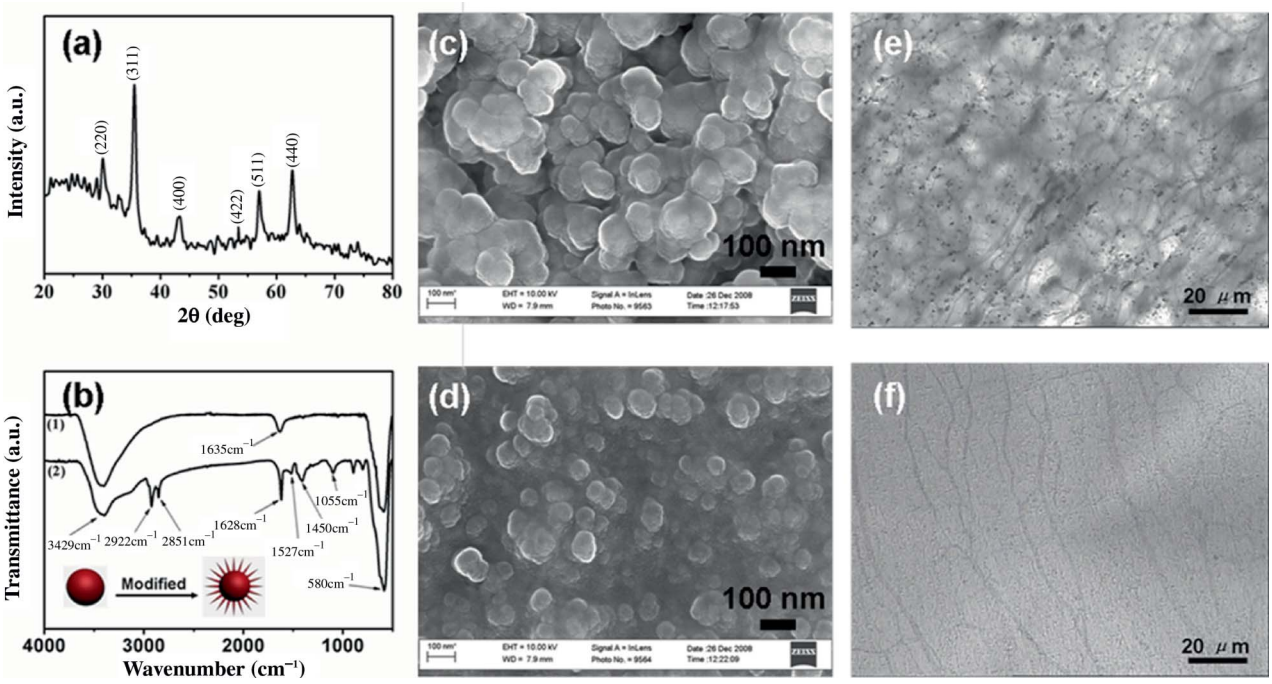

Figure 2. (a) X-ray diffraction curve of the prepared magnetite (Fe_3O_4) sample. (b1) Infrared spectra of the unmodified Fe_3O_4 nanoparticles and (b2) nanoparticles modified by oleic acid. (c) Scanning electron microscopy images of the unmodified Fe_3O_4 nanoparticles and (d) modified nanoparticles. (e) Polarising optical microscopy micrographs of sample 1, the unmodified nanoparticles dispersed in N*-LC and (f) sample 2, the modified nanoparticles.

magnetically in the colour background. If the magnet is placed on the surface of substrate B, the cell will show colour only when observed from the side of substrate A because the Fe_3O_4 nanoparticles have moved to the inner surface of substrate B as shown in Figure 3(c). Then the pattern is erased magnetically. In this way, the modified Fe_3O_4 nanoparticle/N*-LC composite exhibits magnetically addressable and erasable characteristics. Figure 3(d)–(g) shows the photographs of the cell containing sample 2 during the magnetically addressing and erasing process, correspondingly.

However, a problem occurred when more information was required to be addressed in one cell. If two character Ts were 'written' in the cell and the distance between the two Ts was not far enough, some nanoparticles of the first T would move gradually to the area where the magnet existed while the second T was writing, which made the first T rather unclear, as shown in Figure 3(h). In order to solve this problem, a photopolymerisable LC monomer, C6M and photoinitiator, IRG 651, were added and sample 3 was prepared, as shown in Table 1. Then, a photo-mask was put on the cell and the cell was irradiated with UV light (1.45 mW cm^{-2}, 365.0 nm) at 300 K for 20 min. Due to the photo-mask the polymer network could only form in the regions exposed by the UV light, a patterned polymer network, which looked like a 'wall', formed in the cell. Figure 3(i) shows the SEM image of the polymer wall formed in sample 3. Owing to the formation of the polymer wall, the nanoparticles could only move up and down in the specified regions surrounded by the polymer wall and the movement from one region to another one was restricted, as shown schematically in Figure 3(j). After the formation of the polymer wall, as shown in Figure 3(k), two character Ts could be 'written' in the cell clearly; in other words, the resolution in Figure 3(k) is much higher than that in Figure 3(h). Meanwhile, it was demonstrated that the state in Figure 3(k) was stable for over 3 months at room temperature without any external fields, because the high viscosity of the N*-LC could prevent the uniform diffusion of nanoparticles in the composite during this period.

In addition, with this method, a kind of reflective colour information can also be addressed in a reflective colour background. To do that, some CPC, whose chemical structure is shown in Figure 1, was added and samples 4 and 5 were prepared. Then the oleic acid-modified Fe_3O_4 nanoparticles and CPC were mixed thoroughly in appropriate proportions in a non-protic solvent (THF), followed by slow evaporation, and the CPC-modified Fe_3O_4 nanoparticles were obtained [30–32]. Figure 4 shows the IR spectra of the

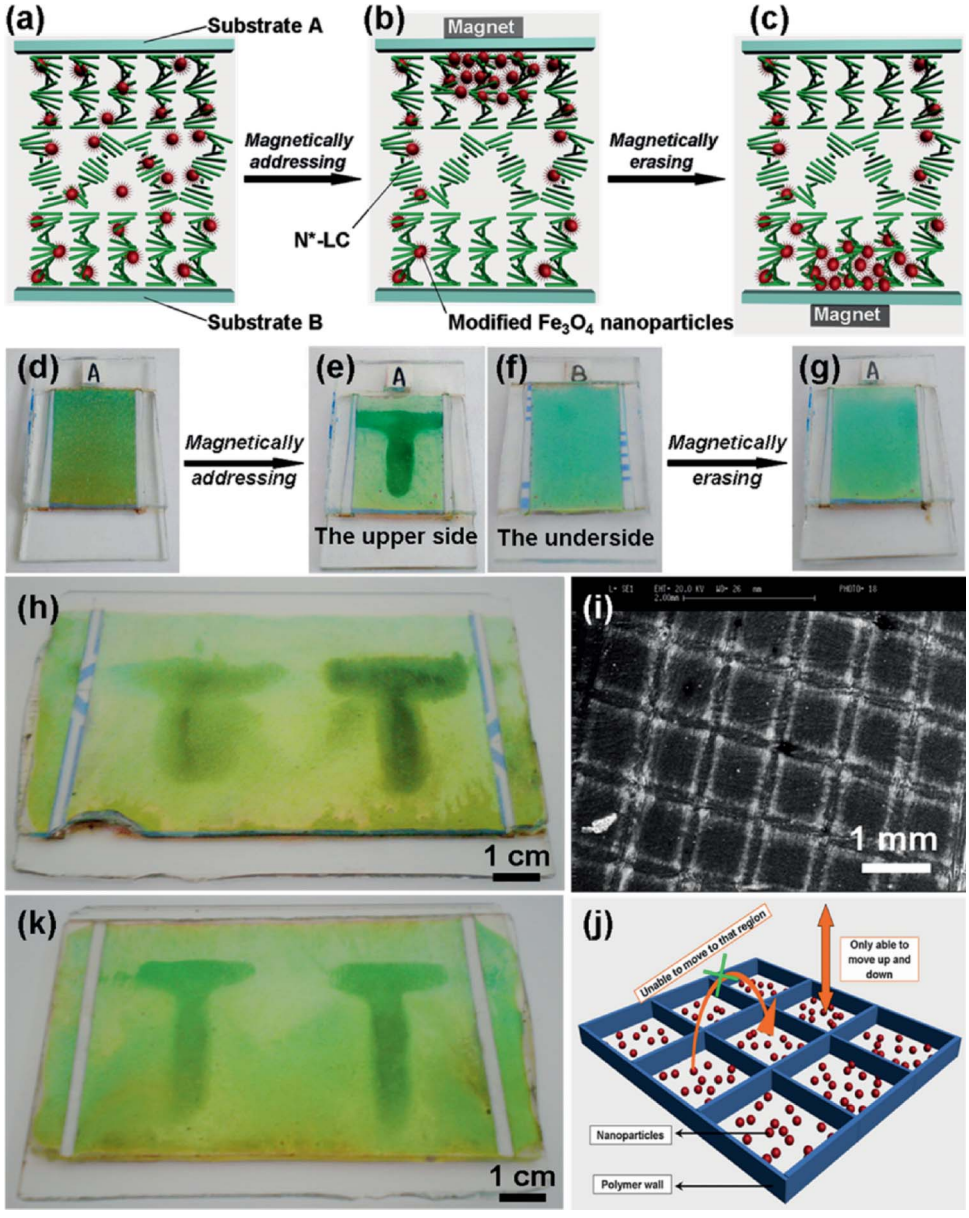

Figure 3. (a)–(c) Schematic mechanism of the composite as M-paper. (d–g) Photographs of the prepared cell containing sample 2 with magnetically addressed and magnetically erased characteristics. (h) Photograph of the cell containing sample 2 without a polymer wall after two character Ts were addressed. (i) Scanning electron microscopy image of a polymer wall network formed in sample 3. (j) Scheme of the role of a polymer wall as it affects the movement of nanoparticles. (k) Photograph of the cell containing sample 3 with a polymer wall after two character Ts were addressed (colour version online).

oleic acid-modified Fe_3O_4 nanoparticles (curve 1) as well as the CPC-modified ones (curve 2), respectively. In spectrum 2, the absorption around 3300 cm^{-1} shows the existence of hydrogen bonds (H-bonds) between the –OH groups on the nanoparticles and pyridine groups of CPC. Moreover, by comparing spectra 1 and 2, it can also be observed that the H-bonds make the absorption of the –OH groups shift somewhat to a shorter wave number, which demonstrates the formation of H-bonds between the modified Fe_3O_4 nanoparticles and CPC molecules [33]. As a result, it can be concluded that the H-bonds should also form between some Fe_3O_4 nanoparticles and CPC molecules in samples 4 and 5. After the cells containing samples 4 and 5 were irradiated with UV light through the photo-mask, polymer walls were also formed in them, as shown schematically in Figure 5(a). A magnet applied to one side of the cell should make the nanoparticles move to the inner surface of substrate A, as shown schematically in Figure 5(b). Meanwhile, some

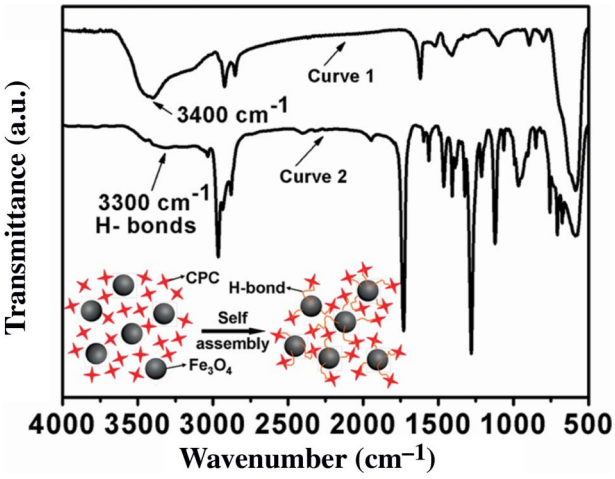

Figure 4. Infrared spectra of the Fe_3O_4 nanoparticles modified by oleic acid (curve 1) and then by chiral pyridine compound (curve 2), respectively.

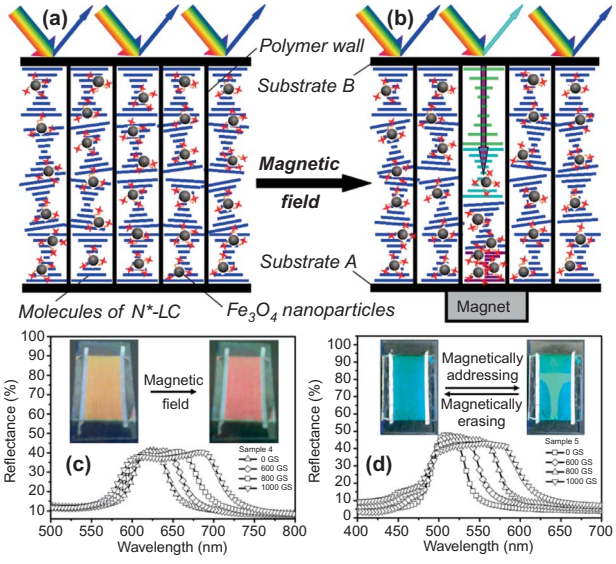

Figure 5. (a) and (b) The schematic mechanism for the expected material as a type of reflective colour M-paper with magnetically controllable characteristics. (c) and (d) The intensity of magnetic field dependence of reflection spectra of samples 4 and 5, as well as the photographs of samples 4 and 5 before and after magnetic fields of 1000 GS were applied, respectively (colour version online).

CPC molecules formed H-bonds with the –OH groups on some nanoparticles and should also move to the inner surface together with the nanoparticles. Consequently, in the region near the surface of substrate B, the density of CPC molecules should decrease and the pitch length of the N*-LC should increase, as shown schematically in Figure 5(b). Thus, a pitch gradient can be formed in the region where the magnetic field is applied and the reflection bandwidth in this region becomes wider than that of other regions. Figure 5(c) and (d) shows the intensity of magnetic field dependence of reflection spectra of samples 4 and 5, respectively. It is not difficult to understand that an increase in magnetic field intensities should result in a greater pitch gradient, which should be the reason why the reflection bandwidths of samples 4 and 5 increase with increasing intensities of the magnetic fields, as shown in Figure 5(c) and (d). Moreover, it can also be seen that the reflection bandwidth can be controlled accurately by adjusting the intensity of the applied magnetic field. When a magnetic field of 1000 GS is applied, the reflection bandwidths of samples 4 and 5 cover the wavelength range of 600–720 nm and 490–600 nm, respectively. The insets in Figure 5(c) show the photographs of sample 4 before and after a magnetic field was applied. It was found that the reflective colour turned from orange to red upon the application of the magnetic field. Meanwhile, it was also proved that such a colour change does not occur in the composite without CPC, which demonstrates that the above explanation of the mechanism is reasonable. In addition, the intensity of the magnetic field applied in our experiment was not high enough to affect the planar texture of the N*-LC [34]. Using the same method, a green character T could also be addressed in a blue background (sample 5) when a magnet of 1000 GS was scanned locally on the cell surface at a speed of 1 cm s^{-1}, as shown in Figure 5(d). Moreover, the magnetochromic effect could be maintained for about 3 months at room temperature without any external fields, thus exhibiting the memory effect.

4. Conclusions

In summary, the magneto-optical characteristics of a Fe_3O_4 nanoparticle/N*-LC composite was studied. The nanoparticles modified by oleic acid could be dispersed much better in the N*-LC. The resolution could be improved in the composite by the preparation of a polymer wall where the composite was used as the material for M-paper. Furthermore, the magneto-chromic characteristics of a Fe_3O_4 nanoparticle/N*-LC composite were shown and the intensity of the driving magnetic field was quite low. After the formation of H-bonds between nanoparticles and the CPC, the pitch length of the N*-LC could be adjusted by altering the intensity of the applied magnetic field and this novel composite could be used as the material for a type of reflective colour M-paper. Both the character (information) and the background of this M-paper exhibited both reflective colours by reflecting visible light around it, backlight was unnecessary and power consumption was low, which must attract more attention in the near future.

Acknowledgements

This study was financially supported by the National Natural Science Foundation of China (Grant No. 20674005 and No. 50725208), Key Program for Panel Display of 863 Program of China (Grant No. 2008AA03A318), State Key Project of Fundamental Research for Nanoscience and Nanotechnology (Grant No. 2006CB932301) and Doctoral Fund of the Ministry of Education of China (Grant No. 20050425850).

References

[1] Comiskey, B.; Albert, J.D.; Yoshizawa, H.; Jacobson, J. *Nature* (London, UK) **1998**, *394*, 253–255.
[2] Hayes, R.A.; Feenstra, B.J. *Nature* (London, UK) **2003**, *425*, 383–385.
[3] Xu, M.; Yang, D.K. *Appl. Phys. Lett.* **1997**, *70*, 720–722.
[4] Hsu, J.S.; Liang, B.J.; Chen, S.H. *Appl. Phys. Lett.* **2004**, *85*, 5511–5513.
[5] Yang, H.; Kikuchi, H.; Kajiyama, T. *Liq. Cryst.* **2000**, *27*, 1695–1699.
[6] Yang, H.; Kikuchi, H.; Kajiyama, T. *Liq. Cryst.* **2002**, *29*, 1141–1149.
[7] Geng, J.; Dong, C.; Zhang, L.P.; Ma, Z.; Shi, L.; Cao, H.; Yang, H. *Appl. Phys. Lett.* **2006**, *89*, 081130.
[8] Yang, D.K.; West, J.L.; Chien, L.C.; Doane, J.W. *J. Appl. Phys.* **1994**, *76*, 1331–1333.
[9] Wu, S.T.; Yang, D.K. Liquid Crystal Materials. In *Reflective Liquid Crystal Displays*; Wiley: New York, 2001; Chapter 1, pp 49.
[10] Xianyu, H.; Faris, S.; Crawford, G.P. *Appl. Opt.* **2004**, *43*, 5006–5015.
[11] Yu, H.P.; Tang, B.Y.; Li, J.H.; Li, L. *Opt. Express* **2005**, *13*, 7243–7249.
[12] Schadt, M.; Gerber, P. *Mol. Cryst. Liq. Cryst.* **1981**, *65*, 241–264.
[13] Xianyu, H.; Lin, T.H.; Wu, S.T. *Appl. Phys. Lett.* **2006**, *89*, 091124.
[14] Furumi, S.; Yokoyama, S.; Otomo, A.; Mashiko, S. *Appl. Phys. Lett.* **2003**, *82*, 16–18.
[15] Chanishvili, A.; Chilaya, G.; Petriashvili, G.; Barberi, R.; Bartolino, R.; Cipparrone, G.; Mazzulla, A.; Oriol, L. *Adv. Mater.* (Weinheim, Ger.) **2004**, *16*, 791–794.
[16] Lin, T.H.; Chen, Y.J.; Wu, C.H.; Fuh, A.Y.G.; Liu, J.H.; Yang, P.C. *Appl. Phys. Lett.* **2005**, *86*, 161120.
[17] Chien, L.C.; Muller, U.; Nabor, M.F.; Doane, J.W. *SID Tech. Digest* **1995**, *26*, 169–171.
[18] Huang, Y.H.; Zhou, Y.; Wu, S.T. *Appl. Phys. Lett.* **2006**, *88*, 011107.
[19] Huang, Y.H.; Zhou, Y.; Doyle, C.; Wu, S.T. *Opt. Express* **2006**, *14*, 1236–1242.
[20] de Gennes, P.G.; Prost, J. Long- and Short-range Order in Nematics. In *The Physics of Liquid Crystals*, 2nd edition; Clarendon: Oxford, 1993; Chapter 2, pp 41.
[21] Broer, D.J.; Boven, J. Mol, G.N.; Challa, G. *Makromol. Chem.* **1989**, *190*, 2255–2268.
[22] Cornell, R.M.; Schwertmann, U. Feroxyhyte. In *The Iron Oxides: Structure, Properties, Reactions, Occurrence and Uses*; Wiley-VCH: New York, 1996; Chapter 7, pp 99.
[23] Saravia, D.C.A.; Bee, A.; Shibli, S.M. *J. Magn. Magn. Mater.* **2005**, *289*, 152–154.
[24] Cheng, F.Y.; Su, C.H.; Yang, Y.S.; Yeh, C.S.; Tsai, C.Y.; Wu, C.L.; Wu, M.T.; Shieh, D.B. *Biomaterials* **2005**, *26*, 729–738.
[25] Liu, Q.X.; Xu, Z.H. *Langmuir* **1995**, *11*, 4617–4622.
[26] Bourlinos, A.B.; Bakandritsos, A.; Georgakilas, V.; Petridis, D. *Chem. Mater.* **2002**, *14*, 3226–3228.
[27] Wang, Y.; Teng, X.W.; Wang, J.S.; Yang, H. *Nano Lett.* **2003**, *3*, 789–793.
[28] Sun, S.H.; Zeng, H.; Robinson, D.B.; Raoux, S.; Rice, P.M.; Wang, S.X.; Li, G.X. *J. Am. Chem. Soc.* **2004**, *126*, 273–279.
[29] Bacri, J.C.; Perzynski, R.; Salin, D. *J. Magn. Magn. Mater.* **1990**, *85*, 27–32.
[30] Kato, T.; Frechet, J.M.J. *J. Am. Chem. Soc.* **1989**, *111*, 8533–8534.
[31] Kato, T.; Frechet, J.M.J.; Wilson, P.G.; Saito, T.; Uryu, T.; Fujishima, A.; Jin, C.; Kaneuchi, F. *Chem. Mater.* **1993**, *5*, 1094–1100.
[32] Osuji, C.; Chao, C.Y.; Bita, I.; Ober, C.K.; Thomas, E.L. *Adv. Funct. Mater.* **2002**, *12*, 753–758.
[33] Odinokov, S.E.; Mashkovsky, A.A.; Glazunov, V.P.; Iogansen, A.V.; Rassadin, B.V. *Spectrochim. Acta* **1976**, *32*, 1355.
[34] de Gennes, P.G.; Prost, J. Defects and Textures in Nematics. In *The Physics of Liquid Crystals*, 2nd edition; Clarendon: Oxford, 1993; Chapter 4, pp 163.